Applied Problems of Nonlinear Oscillation and Wave Theory

Izvestiya Vysshikh Uchebnykh Zavedeniy. Applied Nonlinear Dynamics. 2026;34(2)

Article DOI: 10.18500/0869-6632-003205

Control of the motion of a circular foil using attached sources and internal mechanisms

E. V. Vetchanin✉, *E. M. Artemova*

Ural Mathematical Center, Udmurt State University, Izhevsk, Russia
E-mail: ✉eugene186@mail.ru, liz-artemova2014@yandex.ru
Received 30.08.2025, accepted 17.11.2025, available online 9.12.2025, published 31.03.2026

Abstract. *The purpose* of this paper is to analyze the problem of controlling the plane-parallel motion of a circular foil in an ideal fluid by changing the intensity of attached sources and rotation of the internal rotor. *Methods.* To develop the mathematical model, use is made of the description of fluid motion based on a complex potential, which allows calculation of the fluid forces acting on the moving body. To solve the control problem, the assumption of the piecewise constant form of control actions is made, which allows the equations of motion to be explicitly integrated by analytical methods. *Results.* Equations of the plane-parallel motion of a circular (generally unbalanced) foil with an arbitrary number of attached sources are derived. The motion of the sources relative to the foil and their intensities are given by explicit functions of time. An explicit integration of the equations of motion is performed for the case of a balanced foil with one attached source for piecewise constant controls. *Conclusion.* Explicit solutions to the equations of motion are used to design gaits for in-place turning and forward movement. An algorithm for moving the foil in the neighborhood of a prescribed trajectory by alternately using elementary gaits is formulated. The proposed algorithm of trajectory control is a constructive proof of the controllability of the system considered. The solution to the control problem obtained in this way can be used as a basis for solving the same problem in the case of smooth controls.

Keywords: the motion control, ideal fluid, circular foil, attached source.

Acknowledgements. The work of E.V. Vetchanin was carried out within the framework of the state assignment of the Ministry of Science and Higher Education of Russia (FEWS-2024-0007). The work of E.M. Artemova was performed at the Ural Mathematical Center (Agreement No. 075-02-2025-1609). The authors thank A.A. Kilin and I.Y. Polekhin for discussion of results, and anonymous reviewers for careful reading of the work and valuable comments.

For citation: Vetchanin EV, Artemova EM. Control of the motion of a circular foil using attached sources and internal mechanisms. Izvestiya VUZ. Applied Nonlinear Dynamics. 2026;34(2):223–246. DOI: 10.18500/0869-6632-003205

Introduction

To describe the motion of a rigid body in a fluid, one uses various mathematical models. The most complete description is based on a simultaneous numerical solution of the Newton – Euler equations and the Navier – Stokes equations. This approach is too labor-intensive to carry out an exhaustive analysis of the system's dynamics. However, it allows one to obtain some useful results concerning correction of simple mathematical models [1] or identification of their parameters [2]. We also note that under some assumptions about the motion of a rigid body and its geometry it is possible to carry out a semianalytic investigation based on asymptotic methods [3].

A fairly large class of models describing the plane-parallel motion of a rigid body can be obtained on the basis of the model of an ideal fluid. In particular, this is the model of coupled motion of a circular cylinder and point vortices [4,5]. Recent publications addressed the problem of interaction of a circular cylinder with a fixed point singularity, in particular, with a source [6–8]. In [8] it was shown that in the presence of proper circulation of the cylinder the type of fixed point singularity qualitatively changes the dynamics of the system. Qualitative differences also arise in the case of an elliptic body [9].

In [6–9], the position of the point singularity was assumed to be fixed in some fixed reference frame. Another formulation of the problem is of interest in which the point singularity moves together with the body at some fixed distance from it. Such a problem statement can be found in the recent publication [10], where the motion of a balanced elliptic body with an attached vortex was examined.

In this paper, we address the problem of the plane-parallel motion of a circular foil with a rotor and attached sources. Such a system can be interpreted as the model of a water-jet propulsion device. We will be primarily interested in partial solutions to equations of motion used to perform elementary gaits (turning and propulsion) whose combination will enable an arbitrary transfer of the foil.

1. Mathematical model

Basic notation and assumptions. Consider the plane-parallel motion of an unbalanced circular foil with a rotor in the presence of N point sources in an infinite volume of an ideal incompressible fluid. Assume that the fluid performs potential motion and is at rest at infinity, and its motion about the foil is irrotational.

To derive a mathematical model, we introduce the following notation for the system's parameters:

- m_c — the mass of the foil, kg/m,
- I_c — the central moment of inertia of the foil, kg · m,
- R — the radius of the foil, m,
- σ — the distance between the geometric center of the foil and the center of mass of the foil-rotor system, m,
- m_r — the mass of the rotor, kg/m
- I_r — the central moment of inertia of the rotor, kg · m,
- Ω — the angular velocity of the rotor, which is a given function of time, s^{-1},
- q_n — the intensity of the nth source, which is, in the general case, a given function of time, $n = 1, \ldots, N$, m^2/s.

Since we consider plane-parallel motion, we assume that m_c, m_r, I_c, I_r are quantities per unit length of the foil.

To describe the motion of the system under consideration, we introduce two frames of reference: a fixed (inertial) frame OXY and a moving frame Cxy attached to the foil (see Fig. 1). We assume that the origin of the moving reference frame C is at the geometric center of the foil, and the center of mass of the system lies on the axis Cx.

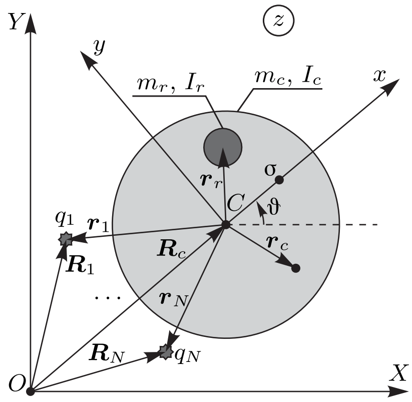

Fig. 1. A schematic representation of an unbalanced circular foil and the point sources.

We will specify the position of the foil relative to the fixed reference frame by the radius vector of its geometric center $\boldsymbol{R}_c = (X_c, Y_c)$, and the orientation of the foil, by angle ϑ between the positive directions of the axes OX and Cx. We will specify the position of the nth source relative to the foil by the radius vector $\boldsymbol{r}_n = (x_n, y_n)$ referred to the moving reference frame. The quantities defining the configuration of the system are shown in Fig. 1.

Remark 1. *The radius vector $\boldsymbol{R}_n = (X_n, Y_n)$, which defines the position of the nth source relative to the fixed reference frame, can be calculated as follows:*

$$\boldsymbol{R}_n = \boldsymbol{R}_c + \begin{pmatrix} \cos\vartheta & -\sin\vartheta \\ \sin\vartheta & \cos\vartheta \end{pmatrix} \boldsymbol{r}_n.$$

The motion of the fluid and the force exerted by it. The motion of the foil is determined by the pressure distribution along its boundary. In the model of the potential flow of an ideal fluid the pressure field, in its turn, is related to the velocity distribution and the potential of the flow by the Cauchy-Lagrange integral [11]. To describe the motion of the fluid, we associate a complex number $z = x + iy$ to each point of the plane Cxy. Then the complex potential of the flow can be written as [11, 12]:

$$W = -\frac{R^2 u}{z} + \sum_{n=1}^{N} \frac{q_n}{2\pi} \ln\left(z - z_n\right) + \sum_{n=1}^{N} \frac{q_n}{2\pi} \ln\left(\frac{R^2}{z} - \overline{z}_n\right), \tag{1}$$

where $z_n = x_n + iy_n$ is the complex-valued function of time that specifies the position of the nth source in the moving reference frame Cxy. The expression (1) contains the complex quantity $u = u_x + iu_y$, which is composed of the projections of the velocity of the geometric center of the foil onto the axes of the reference frame Cxy.

The principal vector of pressure forces (f_x, f_y) acting on the foil, referred to the moving reference frame, can be calculated in complex form using the method proposed in [13]:

$$f_x + if_y = \overline{\frac{i\rho}{2} \oint \left(\frac{dW}{dz}\right)^2 dz} + \frac{d}{dt}\left(\rho \frac{dSZ_c}{dt} + i\rho \oint z \frac{dW}{dz} dz\right). \tag{2}$$

Here, ρ is the density of the fluid, kg/m^3, $S = \pi R^2$ is the area of the foil, integration is performed along its boundary, $\overline{(\cdot)}$ is complex conjugation, and the operator of differentiation with respect to time is defined as follows:

$$\frac{d(\cdot)}{dt} = \left[\frac{\delta}{\delta t} + i\omega\right](\cdot),$$

where the symbol $\dfrac{\delta}{\delta t}$ denotes differentiation with respect to time relative to the moving reference frame rotating with angular velocity ω[1].

Substituting the complex potential (1) into (2) and calculating the integrals, we obtain an explicit representation of the principal vector of pressure forces

$$f_x + if_y = \hat{f}_x + i\hat{f}_y - \rho\pi R^2\dot{u} - i\rho\pi R^2\omega u, \tag{3}$$

$$\hat{f}_x + i\hat{f}_y = -\frac{\rho}{2\pi}\left(\left(\sum_{j=1}^{N} q_j\right)\sum_{n=1}^{N}\frac{q_n z_n}{|z_n|^2} - \sum_{n=1}^{N}\sum_{j=1}^{N}\frac{q_n q_j z_j}{\overline{z}_n z_j - R^2}\right) + \rho R^2\sum_{n=1}^{N} q_n\frac{\overline{u} z_n^2}{|z_n|^4}$$
$$+ \rho R^2\sum_{n=1}^{N} q_n\frac{\dot{\overline{z}}_n z_n^2}{|z_n|^4} - \rho R^2\sum_{n=1}^{N}\dot{q}_n\frac{z_n}{|z_n|^2} - i\rho R^2\omega\sum_{n=1}^{N}\frac{q_n z_n}{|z_n|^2}. \tag{4}$$

The components f_x and f_y calculated in this way are referred to the unit length of the cylinder and have dimension N/m. The last two terms in the expression (3) define the reaction of the fluid to the accelerated motion of the body, i.e., they describe the effect of added masses [14].

Remark 2. *Calculation of the principal vector of pressure forces can also be performed in the real form*

$$f_x = -\oint p\,dy, \quad f_y = \oint p\,dx,$$

where pressure p is determined by the Cauchy–Lagrange integral. However, in practice it is simpler to perform calculations in complex form by the formula (2) constructed using the Cauchy-Lagrange integral.

We note that, for a circular foil, the moment of pressure forces relative to its geometric center is zero. This is due to the fact that the model under consideration does not incorporate tangential stresses, and the lines of action of normal stresses at each point of the boundary of the foil pass through its geometric center.

Equations of motion. Following the approach known from rigid body dynamics [15] for deriving equations of motion, we define the projections p_x and p_y of the linear momentum of the foil-rotor-fluid system onto the moving axes and the angular momentum p_ϑ relative to the geometric center of the foil as

$$p_x = mu_x, \quad p_y = m(u_y + \sigma\omega), \quad p_\vartheta = m\sigma u_y + I\omega + k(t), \tag{5}$$
$$m = m_c + m_r + \rho\pi R^2, \quad I = I_c + m_c(x_c^2 + y_c^2) + I_r + m_r(x_r^2 + y_r^2),$$

where $k(t) = I_r\Omega(t)$ is the angular momentum of the rotor, x_c and y_c are the components of the radius vector $\boldsymbol{r}_c$ of the position of the center of mass of the foil, and x_r and y_r are the components of the radius vector $\boldsymbol{r}_r$ of the position of the center of mass of the rotor. Note that the effect of added masses is taken into account as additional linear momentum, and that the added mass itself is included in the effective mass m as a third term.

[1]We note that the formula (2) does not contain the translational velocity of the moving reference frame since the motion of the foil is assumed to be irrotational. However, after explicit calculations of the corresponding integrals, the translational velocity components and their derivatives will arise in the expressions for the forces.

With the notation introduced above and the choice of reference frames, the equations of motion of the foil can be represented as the Newton – Euler equations:

$$\dot{p}_x = p_y\omega + \hat{f}_x, \quad \dot{p}_y = -p_x\omega + \hat{f}_y, \quad \dot{p}_\vartheta = p_x u_y - p_y u_x, \tag{6}$$
$$u_x = \frac{p_x}{m}, \quad u_y = \frac{Ip_y - m\sigma(p_\vartheta - k(t))}{m(I - m\sigma^2)}, \quad \omega = \frac{-\sigma p_y + p_\vartheta - k(t)}{I - m\sigma^2}.$$

Since the expressions for $\hat{f}_x$ and $\hat{f}_y$ depend on the velocities u_x, u_y, ω and the positions and intensities of the sources are assumed to be given functions of time, equations (6) form a closed system of equations.

We supplement (6) with the kinematic relations

$$\dot{Z}_c = ue^{i\vartheta}, \quad \dot{\vartheta} = \omega \tag{7}$$

to reconstruct the trajectory of the foil in absolute space. Here $Z_c = X_c + iY_c$ is the complex coordinate of the geometric center of the foil in the fixed reference frame.

Next, for the system described above, we consider the following control problem:

move the foil from the initial point to the end point near a given trajectory by changing the intensities q_n of the attached sources (in particular, of one source) and the angular momentum of the rotor $k(t)$. At the initial and terminal instants of motion we require that the system be at rest ($u_x = u_y = 0$, $\omega = 0$, $k = 0$, $q_n = 0$, $n = 1, \ldots, N$).

We note that the attached source may be regarded as a simplified model of a water-jet engine. The positive intensity corresponds to the fluid discharge performed by the engine, the negative intensity corresponds to the fluid intake, and the zero intensity corresponds to the switched-off engine.

2. Exact solutions to the equations of motion for a balanced foil with one source

The simplest case for analytic investigation and further construction of the control algorithm is that of a balanced foil ($\sigma = 0$), in particular, with one attached source on the positive part of the axis Cx, i.e., $z_1 = r > R$, where r is the distance between the geometric center of the foil and the source (see Fig. 2).

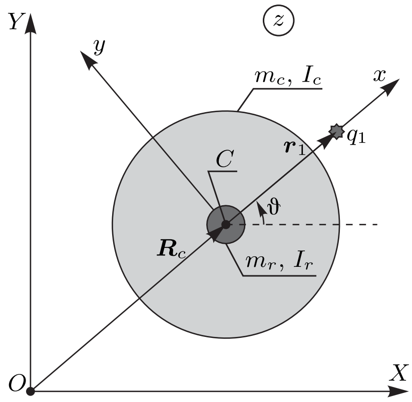

Fig. 2. A schematic representation of a balanced circular foil and an attached point source

To write the equations of motion in a more compact form, we perform the renormalization

$$\frac{\rho R^2 q_1}{mr^2} \mapsto q_1, \tag{8}$$

then equations (6) and the kinematic relations (7) take the form

$$\dot{p}_x = q_1 p_x + \omega p_y + \beta q_1^2 - mr\dot{q}_1, \quad \dot{p}_y = -\omega p_x - q_1 p_y - mrq_1\omega, \quad \dot{p}_\vartheta = 0, \tag{9}$$

$$\dot{Z}_c = m^{-1}(p_x + ip_y)e^{i\vartheta}, \tag{10}$$

$$\dot{\vartheta} = \omega. \tag{11}$$

Here, $\omega = I^{-1}\big(p_\vartheta - k(t)\big)$, $\beta = \dfrac{m^2 r^3}{2\pi\rho R^2(r^2 - R^2)}$.

From the third of equations (9) we see that p_ϑ is a first integral:

$$p_\vartheta = f = \text{const}, \tag{12}$$

and the zero level set of this integral corresponds to motion from the state of rest ($\omega = 0$, $k = 0$). The existence of the first integral (12) allows one to consider, instead of $k(t)$, the angular velocity $\omega(t)$ as a new control.

Next, we consider piecewise constant controls, which in the general case can be written as

$$\begin{pmatrix} q_1 \\ \omega \end{pmatrix} = \sum_{j=1}^{M} \begin{pmatrix} Q_j \\ \Omega_j \end{pmatrix} \big(\Theta(t - \tau_j) - \Theta(t - \tau_{j+1})\big), \quad Q_j = \text{const}, \quad \Omega_{\rm j} = \text{const}, \tag{13}$$

where $\Theta(t)$ is the Heaviside function, Q_j, Ω_j are the values of the control actions (the intensity of the source and the angular velocity of the body, respectively) in the time interval $t \in (\tau_j, \tau_{j+1})$, $j = 1, \ldots, M$.

Then, firstly, integration of the first of equations (9) in the intervals $t \in [\tau_j - \varepsilon, \tau_j + \varepsilon]$ as $\varepsilon \to 0$ shows that the linear momentum p_x at time instants τ_j will change abruptly:

$$p_x(\tau_j + 0) = p_x(\tau_j - 0) - mr(Q_j - Q_{j-1}). \tag{14}$$

Secondly, in the time intervals $(\tau_j, \tau_{j+1}]$ equation (11), which governs the evolution of angle ϑ, is integrated trivially:

$$\vartheta(t) = \vartheta(\tau_j) + \Omega_j(t - \tau_j), \quad t \in (\tau_j, \tau_{j+1}]. \tag{15}$$

Thirdly, in the time intervals $(\tau_j, \tau_{j+1}]$ the system (9) becomes a linear inhomogeneous ODE system with constant coefficients whose matrix form is

$$\dot{\boldsymbol{p}} = \mathbf{J}\boldsymbol{p} + \boldsymbol{b}, \quad t \in (\tau_j, \tau_{j+1}], \tag{16}$$

$$\boldsymbol{p} = \begin{pmatrix} p_x \\ p_y \end{pmatrix}, \quad \mathbf{J} = \begin{pmatrix} Q_j & \Omega_j \\ -\Omega_j & -Q_j \end{pmatrix}, \quad \boldsymbol{b} = \begin{pmatrix} \beta Q_j^2 \\ -mrQ_j\Omega_j \end{pmatrix}.$$

The explicit solution of equations (16), together with (15), allows one to integrate the equation of motion of the geometric center of the foil (10) and to find its motion in absolute space.

The form of the solution to equations (16) is defined by the eigenvalues of the matrix $\mathbf{J}$ (for brevity, we omit the index j for Q and Ω here and in what follows):

$$\lambda^2 = \alpha = Q^2 - \Omega^2 = -\det \mathbf{J}. \tag{17}$$

Three qualitatively different cases are possible: *the hyperbolic case* $\alpha > 0$, the *elliptic case* $\alpha < 0$ and the *degenerate case* $\alpha = 0$. Let us find the fixed points of equations (16), their explicit solutions, as well as the trajectories of the geometric center of the foil which correspond to these solutions.

Fixed points of the system. When $\alpha \neq 0$ the matrix $\mathbf{J}$ is nondegenerate and the system (16) always has a fixed point:

$$\boldsymbol{p}^* = -\mathbf{J}^{-1}\boldsymbol{b} = -\frac{mrQ}{\alpha}\begin{pmatrix}\alpha - C^*Q^2\\ C^*\Omega Q\end{pmatrix}, \quad C^* = 1 - \frac{\beta}{mr} = 1 - \frac{mr^2}{2\pi\rho R^2(r^2 - R^2)}, \tag{18}$$

which is a saddle point for $\alpha > 0$ and an elliptic point for $\alpha < 0$.

In the general case, as $\alpha \to 0$, the fixed point (18) goes to infinity. However, if the parameters of the system are such that $C^* = 0$ (for example, if $m = \rho\pi R^2$ and $r = \sqrt{2}R$), then the coordinates of the fixed point will be finite:

$$\boldsymbol{p}^* = \begin{pmatrix}-mrQ\\ 0\end{pmatrix}. \tag{19}$$

In the **hyperbolic case** (with $\alpha > 0$) the eigenvalues of the matrix $\mathbf{J}$ are real. The solution to equations (16) and (10) can be written as

$$\boldsymbol{p}(t) = \boldsymbol{p}^* + C_1\begin{pmatrix}Q + s\sqrt{\alpha}\\ -\Omega\end{pmatrix}e^{s\sqrt{\alpha}(t-\tau)} + C_2\begin{pmatrix}\Omega\\ -Q - s\sqrt{\alpha}\end{pmatrix}e^{-s\sqrt{\alpha}(t-\tau)}, \tag{20}$$

$$\begin{pmatrix}C_1\\ C_2\end{pmatrix} = -\frac{1}{2(\alpha + sQ\sqrt{\alpha})}\begin{pmatrix}-Q - s\sqrt{\alpha} & -\Omega\\ \Omega & Q + s\sqrt{\alpha}\end{pmatrix}(\boldsymbol{p}(\tau) - \boldsymbol{p}^*), \quad s = \operatorname{sign} Q,$$

$$Z(t) = Z(\tau) + e^{i\vartheta(\tau)}\Bigg(Z^* + \frac{C_1(Q + s\sqrt{\alpha} - i\Omega)}{m(s\sqrt{\alpha} + i\Omega)}\left(e^{(s\sqrt{\alpha}+i\Omega)(t-\tau)} - 1\right) + \\ + \frac{C_2(\Omega - i(Q + s\sqrt{\alpha}))}{m(-s\sqrt{\alpha} + i\Omega)}\left(e^{(-s\sqrt{\alpha}+i\Omega)(t-\tau)} - 1\right)\Bigg), \tag{21}$$

where

$$Z^* = \frac{p_x^* + ip_y^*}{m}\begin{cases}\dfrac{e^{i\Omega(t-\tau)} - 1}{i\Omega}, & \Omega \neq 0,\\ t - \tau, & \Omega = 0.\end{cases}$$

This case will be considered in detail in Section 3.

In the **elliptic case** (with $\alpha < 0$) the eigenvalues of the matrix $\mathbf{J}$ are purely imaginary. The solution to equations (16) and (10) can be written as

$$\boldsymbol{p}(t) = \boldsymbol{p}^* + \begin{pmatrix}C_1\Omega\\ -C_1Q + C_2\sqrt{|\alpha|}\end{pmatrix}\cos\sqrt{|\alpha|}(t-\tau) + \begin{pmatrix}C_2\Omega\\ -C_2Q - C_1\sqrt{|\alpha|}\end{pmatrix}\sin\sqrt{|\alpha|}(t-\tau), \tag{22}$$

$$\begin{pmatrix}C_1\\ C_2\end{pmatrix} = \frac{1}{\Omega\sqrt{|\alpha|}}\begin{pmatrix}\sqrt{|\alpha|} & 0\\ Q & \Omega\end{pmatrix}(\boldsymbol{p}(\tau) - \boldsymbol{p}^*).$$

$$Z(t) = Z(\tau) + e^{i\vartheta(\tau)}\Bigg(\frac{p_x^* + ip_y^*}{i\Omega m}\left(e^{i\Omega(t-\tau)} - 1\right) + \frac{C_1 - iC_2}{2}\cdot\frac{\Omega - \sqrt{|\alpha|} - iQ}{m}\cdot\frac{e^{i(\Omega+\sqrt{|\alpha|})(t-\tau)} - 1}{i(\Omega + \sqrt{|\alpha|})} + \\ + \frac{C_1 + iC_2}{2}\cdot\frac{\Omega + \sqrt{|\alpha|} - iQ}{m}\cdot\frac{e^{i(\Omega-\sqrt{|\alpha|})(t-\tau)} - 1}{i(\Omega - \sqrt{|\alpha|})}\Bigg). \tag{23}$$

This case will be studied in detail in Section 4.

In the **degenerate case** (with $\alpha = 0$) the matrix $\mathbf{J}$ has a double zero eigenvalue. The solution to equations (16) and (10) can be written as

$$\boldsymbol{p}(t) = \left(\frac{\Omega(b_1 + sb_2)t^2}{2} + \Omega C_1 t - C_2\right)\begin{pmatrix} s \\ -1 \end{pmatrix} + \boldsymbol{b}t + \begin{pmatrix} C_1 \\ 0 \end{pmatrix}, \quad s = \operatorname{sign}\Omega Q, \tag{24}$$
$$C_1 = p_x(0) + sp_y(0), \quad C_2 = p_y(0).$$

$$Z(t) = Z(0) + e^{i\vartheta(\tau)}\left(\frac{\Omega(b_1 + sb_2)}{2}\cdot\frac{s-i}{m}\left(\left(\frac{(t-\tau)^2}{i\Omega} + \frac{2(t-\tau)}{\Omega^2} - \frac{2}{i\Omega^3}\right)e^{i\Omega(t-\tau)} + \frac{2}{i\Omega^3}\right) + \right.$$
$$+ \frac{\Omega C_1(s-i) + b_1 + ib_2}{m}\left(\left(\frac{(t-\tau)}{i\Omega} + \frac{1}{\Omega^2}\right)e^{i\Omega(t-\tau)} - \frac{1}{\Omega^2}\right) +$$
$$\left. + \frac{-C_2(s-i) + C_1}{m}\left(\frac{1}{i\Omega}e^{i\Omega(t-\tau)} - \frac{1}{i\Omega}\right)\right). \tag{25}$$

The solution (24), (25) is only presented to make the picture complete, and will not be considered in what follows.

3. Analysis of the hyperbolic case

3.1. The main properties of the solution. In the hyperbolic case, one of the components of the linear momentum of the foil $\boldsymbol{p} = (p_x, p_y)$ undergoes an exponential growth, and the solution (20) is unstable to small perturbations. In addition, all trajectories (21) of the geometric center of the foil are noncompact. Therefore, it is impossible to perform an on-the-spot turn of the foil without displacing its geometric center.

We consider separately the case

$$Q < 0, \quad \Omega = 0, \quad p_y = 0, \tag{26}$$

in which the linear momentum vector evolves along the stable separatrix of the fixed saddle point (18). In this case, rectilinear motion occurs without unlimited increase in the velocity, i.e., it is possible to perform a *propulsion gait*, which will be discussed in the next subsection.

3.2. Propulsion gait. Despite the instability (with respect to small perturbations of p_y) of motion along the separatrix $p_y = 0$, we will present conditions under which one can apply it as a *propulsion gait*.

On the invariant manifold $p_y = 0$ (with $\omega = 0$) the equations governing the evolution of p_x takes the form

$$\dot{p}_x = q_1 p_x + \beta q_1^2 - mr\dot{q}_1. \tag{27}$$

Assume that the foil moves during the time interval $t \in [0, T]$ under the action of some control $q_1(t)$, in particular, piecewise constant control. At the initial and terminal instants of time, the following conditions must be satisfied:

$$p_x(+0) = -mrq_1(+0), \quad p_x(T-0) = mrq_1(T-0), \tag{28}$$

i.e., before the control begins to act, the foil is at rest, and when the control is switched off (zeroed instantly) the foil is brought to the state of rest.

It turns out that the second of conditions (28) cannot be satisfied whatever the control law $q_1(t)$. To show this, we perform the following changes of variables:

$$P = p_x + mrq_1, \quad q_1 = \dot{G}, \tag{29}$$

then equation (27) and conditions (28) take the form

$$\dot{P} = \dot{G}P + (\beta - mr)\dot{G}^2, \tag{30}$$

$$P(0) = P(T) = 0. \tag{31}$$

Here, G is any primitive function of q_1. We recall that $\beta = \dfrac{m^2 r^3}{2\pi\rho R^2(r^2 - R^2)}$.

The solution to equation (30) can be represented by the following quadrature:

$$P = (\beta - mr)\int_0^t \dot{G}^2(\tau)e^{G(t)-G(\tau)}d\tau. \tag{32}$$

The initial condition $P(0) = 0$ is fulfilled automatically. But since the integrand in (32) is nonnegative, $P(t) \neq 0$ for any $t > 0$ and $\beta - mr \neq 0$.

Thus, the use of motion on the invariant manifold $p_y = 0$ (with $\omega = 0$) as a *propulsion gait* is only possible if the system's parameters satisfy the relation

$$\beta - mr = 0. \tag{33}$$

We note that condition (33) is equivalent to vanishing of the quantity C^* defined in (18) and, as noted above, it is satisfied, for example, for $m = \rho\pi R^2$ and $r = \sqrt{2}R$.

4. Analysis of the elliptic case

4.1. The main properties of the solution Consider the solution (22), which describes changes in the linear momenta p_x and p_y, under the condition that the motion starts from rest ($p_x(-0) = p_y(-0) = 0$) under the action of control

$$q_1 = Q\Theta(t), \quad \omega = \Omega\Theta(t), \quad Q = \text{const}, \quad \Omega = \text{const}, \tag{34}$$

i.e., in the expression (13) we set $M = 1$, $Q_1 = Q$, $\Omega_1 = \Omega$, $\tau_1 = 0$, $\tau_2 \to +\infty$.

For the above conditions with $t > 0$ the expression (22) defines, depending on the signs of Q and Ω, four periodic functions of time with period $T = \dfrac{2\pi}{\sqrt{|\alpha|}}$ that are symmetric with respect to the axes $p_x = 0$, $p_y = 0$ (see Fig. 3). In some cases, we will call these solutions *cycles* for brevity. By virtue of (14), time $t = +0$ corresponds to the point

$$p_x = -mrQ, \quad p_y = 0. \tag{35}$$

For the cycles described above, the geometric center of the foil moves either along a quasi-periodic or a periodic trajectory (see Fig.4). Periodic motions occur if the frequencies Ω, $\Omega+\sqrt{|\alpha|}$ and $\Omega - \sqrt{|\alpha|}$ in the expression (23) are Diophantine. This arises if the parameters Q and Ω of the control (34) are related by

$$Q^2 = \left(1 - \frac{j^2}{n^2}\right)\Omega^2, \quad j, n \in \mathbb{N}, \quad j < n. \tag{36}$$

In this case, the period of revolution along the trajectory is $T_Z = \dfrac{2\pi n}{\Omega} = \dfrac{2\pi(n \pm j)}{\Omega \pm \sqrt{|\alpha|}}$.

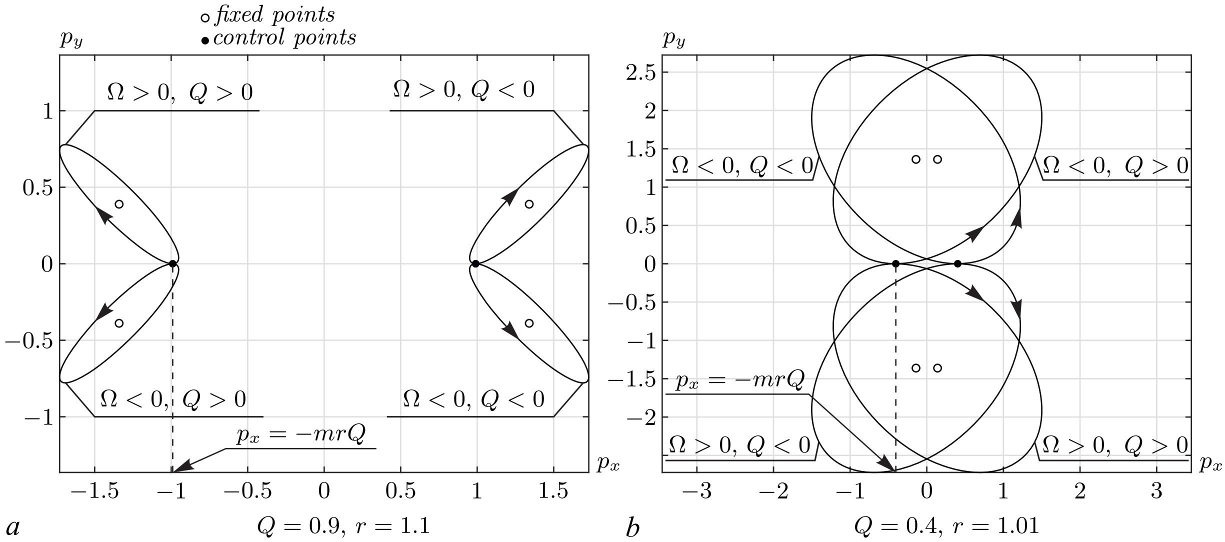

Fig. 3. Examples of symmetric periodic solutions given by (22), under the control (34). Parameter values: $\rho = 1$, $m = 1$, $R = 1$

4.2. On-the-spot turn gait It was noted above that in the general case the trajectories of the geometric center of the foil are compact (see examples in Fig. 4). A special case is $Q = 0$, when one of the frequencies $\Omega \pm \sqrt{|\alpha|}$ that appear in the expression for the trajectory (23) vanishes.

For $Q = 0$ the solution (22), (23) takes the form

$$\boldsymbol{p}(t) = \begin{pmatrix} \cos\omega(t-\tau) & \sin\omega(t-\tau) \\ -\sin\omega(t-\tau) & \cos\omega(t-\tau) \end{pmatrix} \boldsymbol{p}(\tau), \tag{37}$$

$$Z(t) = Z(\tau) + e^{i\vartheta(\tau)} \frac{p_x(\tau) + ip_y(\tau)}{m}(t-\tau), \tag{38}$$

$$\vartheta(t) = \vartheta(\tau) + \omega(t-\tau), \tag{39}$$

which corresponds to the uniform rotation of the foil about its geometric center that moves in a straight line with a constant velocity. Here τ is some initial time instant.

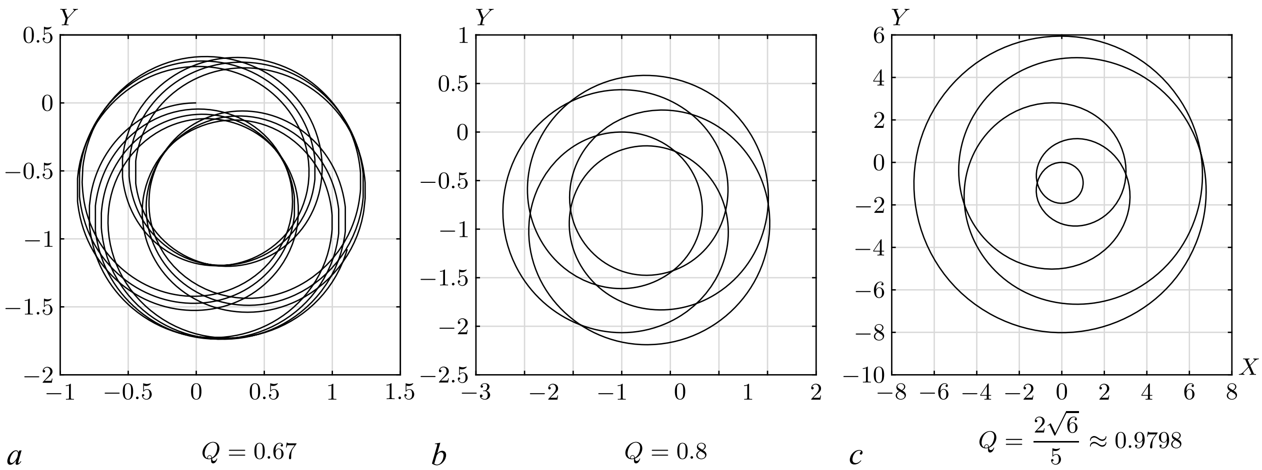

Fig. 4. Examples of trajectories for $\Omega = 1$ and different values of Q. Parameter values: $m = 1$, $I = 0.5$, $\rho = 1$, $R = 1$, $r = 1.1$, $\vartheta(0) = 0$

In the particular case with $\boldsymbol{p}(\tau) = 0$ the foil will uniformly rotate about the fixed geometric center. This mode of motion can be used as a *gait for changing the orientation of the foil.* Physically this gait is performed only by rotating the rotor and is based on the law of conservation of the angular momentum of the system (12). Using relation (12), one can find the angular momentum of the rotor k (and hence its angular velocity $\boldsymbol{\Omega}$), which ensures the rotation of the foil with the required angular velocity ω.

Remark 3. *We note that, in the elliptic case, noncompact trajectories are possible only when the intensity of the source is zero. We write the resonance condition, i.e., for vanishing of the frequencies* $\Omega \pm \sqrt{|\alpha|}$ *that appear in* (23)*:*

$$\Omega \pm \sqrt{|\alpha|} = \Omega \pm \sqrt{\Omega^2 - Q^2} = \frac{Q^2}{\Omega \mp \sqrt{\Omega^2 - Q^2}} = 0.$$

The resulting expression vanishes only for $Q = 0$.

4.3. Propulsion gaits The periodicity of changes in the linear momenta (22) and the symmetry of this solution with respect to the change of signs of Q and $\boldsymbol{\Omega}$ allow several *propulsion gaits* to be performed. We begin by discussing the simplest gait.

1. Consider a control action of the form[2]

$$\begin{pmatrix} q_1 \\ \omega \end{pmatrix} = \big(\Theta(t) - \Theta(t-T)\big)\begin{pmatrix} Q \\ \Omega \end{pmatrix}, \quad Q = \mathrm{const}, \quad \boldsymbol{\Omega} = \mathrm{const}, \quad T = \frac{2\pi}{\sqrt{|\alpha|}}, \tag{40}$$

whose duration coincides with period T of variation of the linear momenta p_x and p_y. For definiteness, we will assume that $Q > 0$ and $\boldsymbol{\Omega} > 0$.

If the foil is at rest before the control is switched on, then by virtue of (14), when $t = 0$, the linear momentum undergoes an abrupt change and takes the value

$$\boldsymbol{p}(+0) = (-mrQ,\, 0)\,. \tag{41}$$

Then, for the duration of the control action, the vector $\boldsymbol{p}$ will trace out an elliptic curve and return to the value (41). When $t = T$, the control actions (40) vanish, and the first component of the linear momentum vector undergoes an abrupt change by the value

$$\boldsymbol{p}(T+0) = \boldsymbol{p}(T-0) + (mrQ,\, 0) \tag{42}$$

which will bring the foil to the state of rest. All the above-mentioned steps of changes in the linear momentum vector are illustrated in Fig. 5.

Next, using (23), we calculate the displacement of the geometric center of the foil under the control (40). It turns out that this quantity can be written as a function of the ratio $g = Q/\boldsymbol{\Omega}$:

$$\begin{gathered} \Delta Z = Z(T) - Z(0) = 2\sigma \exp\left(i\left(\vartheta(0) + \frac{\pi}{\sqrt{1-g^2}} + \frac{\pi}{2}\right)\right)\sin\frac{\pi}{\sqrt{1-g^2}}, \\ \sigma = r\left(\frac{2mr^2 - 4\pi\rho R^2(r^2 - R^2)}{2\pi\rho R^2(r^2 - R^2)} + i\frac{mr^2 g}{2\pi\rho R^2(r^2 - R^2)}\right). \end{gathered} \tag{43}$$

[2]This control law is obtained if we set $M = 1$, $Q_1 = Q$, $\Omega_1 = \Omega$, $\tau_1 = 0$, $\tau_2 = T$ in (13).

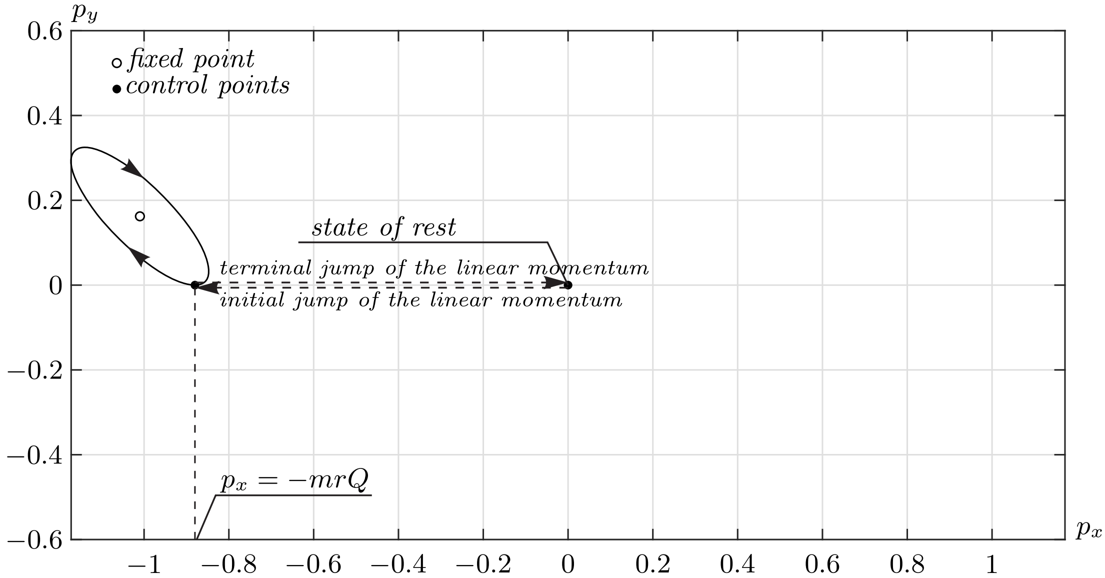

Fig. 5. Changes in the linear momentum vector under the control (40). Parameter values: $m = 1$, $\rho = 1$, $R = 1$, $r = 1.1$, $Q = 0.8$, $\Omega = 1$

Figure 6 shows the dependence of $|\Delta Z|$ on g, as well as examples of trajectories of the geometric center of the foil for some values of g. The value of $|\Delta Z|$ vanishes when

$$g = \frac{\sqrt{n^2 - 1}}{n}, \quad n = 1, 2, \ldots, \tag{44}$$

which corresponds to relation (36) with $j = 1$ and $n > 1$. The value $n = 1$ corresponds to the on-the-spot gait. This dependence has a countable number of maxima. Let g_{max} denote the position of the first maximum, and S_{max}, the corresponding value of propulsion.

We see that by choosing values of Q and Ω one can displace the geometric center of the foil in a given direction by a given distance that does not exceed some limiting value. In particular, in the examples presented in Section 5 we will consider only the case where $g \in [0, g_{max}]$. Also, it can be seen from (43) that the direction of motion can be given by choosing the initial orientation of the foil $\vartheta(0)$.

Thus, the above-described motion, which arises under the action of control (40) can be used as a *propulsion gait*.

2. To construct another propulsion gait, we turn to the symmetry of the solution (22) with respect to the change of sign Q. For definiteness, we will assume $\Omega > 0$. The transition between the cycles depicted in the upper half-plane in Fig. 3, *a* or in the lower half-plane in Fig. 3, *b* can be performed by changing the sign of Q (for definiteness, from the positive to the negative sign) when using a piecewise constant control of the form[3]:

$$\begin{gathered} q_1 = Q\left(\Theta(t) - \Theta(t - t_s)\right) - Q\left(\Theta(t - t_s) - \Theta(t - 2t_s)\right), \\ \omega = \Omega\left(\Theta(t) - \Theta(t - 2t_s)\right). \end{gathered} \tag{45}$$

[3]This control law is obtained if we set $M = 2$, $Q_1 = Q$, $Q_2 = -Q$, $\Omega_1 = \Omega_2 = \Omega$, $\tau_1 = 0$, $\tau_2 = t_s$, $\tau_3 = 2t_s$ in (13).

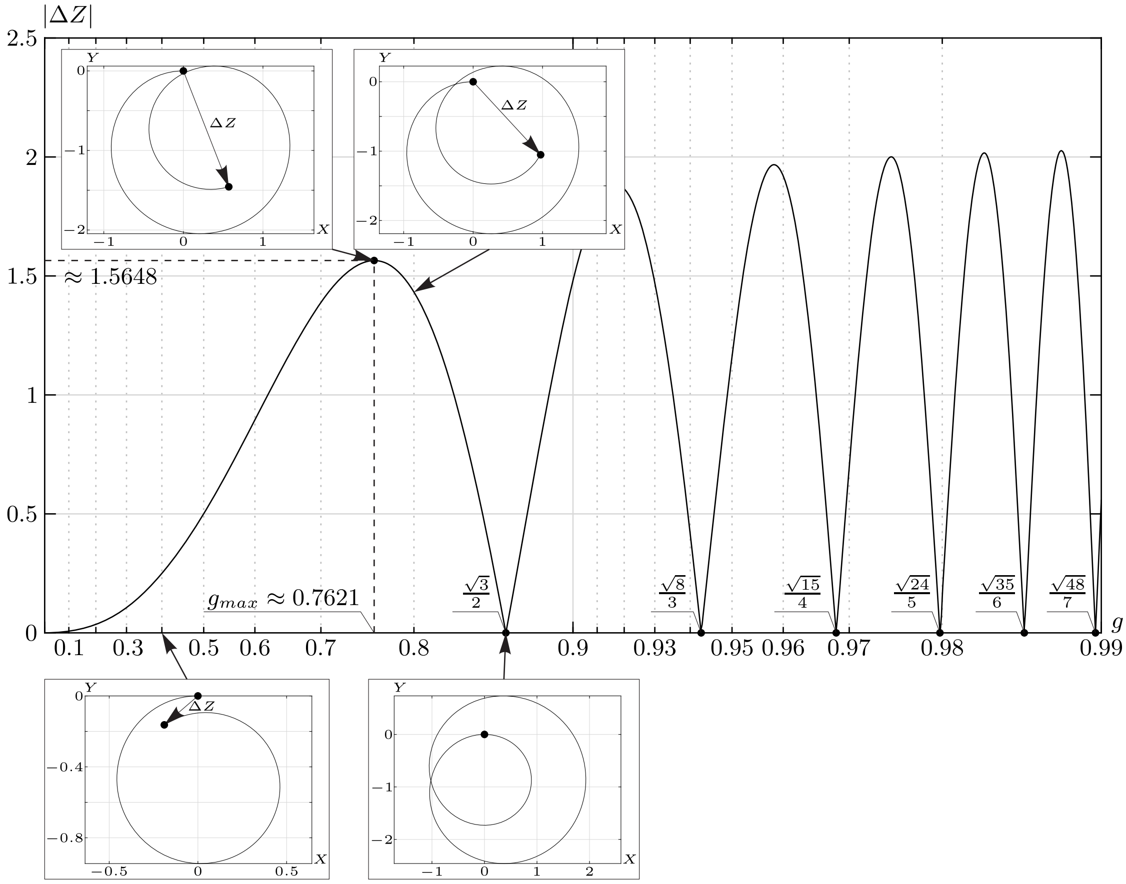

Fig. 6. Dependence of $|\Delta Z|$ on g and examples of trajectories of the geometric center of the foil for the control (40). Parameter values: $m = 1$, $\rho = 1$, $R = 1$, $r = 1.1$, $\vartheta(0) = 0$

Here, the switching time t_s is found from the condition $p_x(t_s)\Big|_{Q>0,\,\Omega>0} = -mrQ$ and is given by the expression

$$t_s = \frac{2}{\sqrt{|\alpha|}}\left(\pi - \arctan\frac{\sqrt{|\alpha|}}{Q}\right). \tag{46}$$

At the initial time instant, when control (45) is switched on, the linear momentum of the foil takes the value

$$\boldsymbol{p} = (-mrQ,\, 0), \tag{47}$$

which during the time interval $t \in (0,\, t_s)$ changes continuously according to the law (22). At time $t = t_s$ the component of the linear momentum p_x takes its initial value, but as q_1 changes sign, it takes the increment

$$p_x(t_s + 0) = p_x(t_s - 0) + 2mrQ = mrQ \tag{48}$$

and reverses sign. Here, a transition to the cycle symmetric to the preceding one occurs. On this cycle, the motion occurs during the time interval $t \in (t_s,\, 2t_s)$ at the end of which the linear momentum takes the value

$$\boldsymbol{p} = (mrQ,\, 0). \tag{49}$$

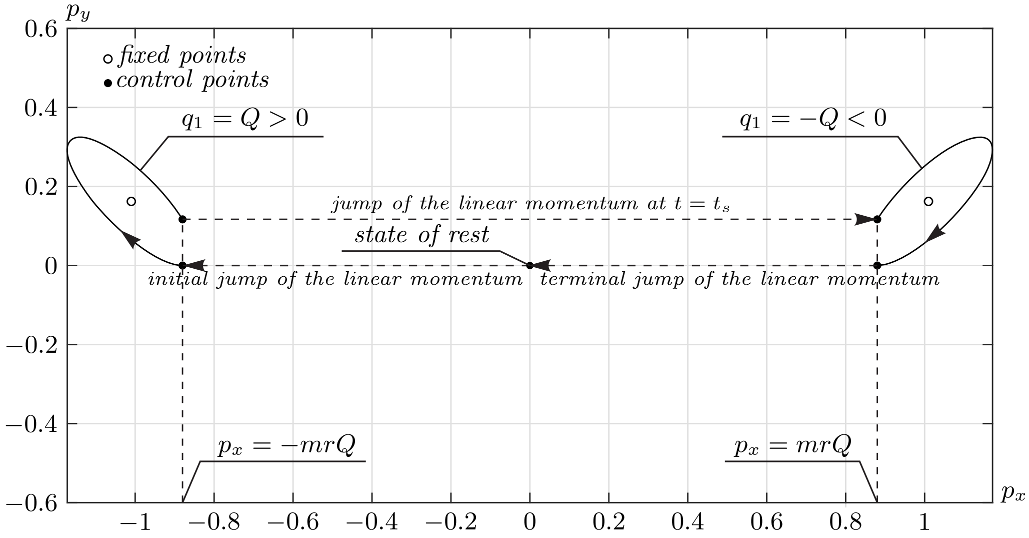

Fig. 7. Changes in the linear momentum vector under the control (45). Parameter values: $m = 1$, $\rho = 1$, $R = 1$, $r = 1.1$, $Q = 0.8$, $\Omega = 1$

At time $t = 2t_s$, the values of the control actions vanish. As a result, the component of the linear momentum p_x undergoes an abrupt change

$$p_x(2t_s + 0) = p_x(2t_s - 0) - mrQ = 0, \tag{50}$$

and the foil comes to the state of rest. The above-described steps of changes in the linear momenta are illustrated in Fig. 7.

Due to the abrupt change in p_x, the trajectory of the geometric center of the foil for the control (45) will have a cusp point. The analytic expression for the dependence of the displacement ΔZ on g has a more cumbersome form and so is not presented here. Figure 8 shows the dependence of $|\Delta Z|$ on g. Compared to the preceding choice of control, this dependence has a more complex form. The zeroes of $|\Delta Z|$ correspond to periodic motions of the geometric center of the foil. Figure 8 also gives examples of trajectories that arise at some values of g.

As can be seen from Fig. 8, the control (45) allows moving the foil over a given distance by an appropriate choice of values of Q and Ω. The required direction of motion is enabled by choosing the angle $\vartheta(0)$.

Remark 4. *If the sign of the angular velocity in the controls (45) is reversed:*

$$\begin{gathered} q_1 = Q\left(\Theta(t) - \Theta(t - t_s)\right) - Q\left(\Theta(t - t_s) - \Theta(t - 2t_s)\right), \quad Q > 0, \\ \omega = -\Omega\left(\Theta(t) - \Theta(t - 2t_s)\right), \quad \Omega > 0 \end{gathered} \tag{51}$$

we obtain a gait similar to that described above.

3. As the sign of q_1 in the control (45) is reversed, i.e.,[4]

$$\begin{gathered} q_1 = -Q\left(\Theta(t) - \Theta(t - t_s)\right) + Q\left(\Theta(t - t_s) - \Theta(t - 2t_s)\right), \quad Q > 0, \\ \omega = \Omega\left(\Theta(t) - \Theta(t - 2t_s)\right), \quad \Omega > 0 \end{gathered} \tag{52}$$

[4]This control law is obtained if we set $M = 2$, $Q_1 = -Q$, $Q_2 = Q$, $\Omega_1 = \Omega_2 = \Omega$, $\tau_1 = 0$, $\tau_2 = t_s$, $\tau_3 = 2t_s$ in (13).

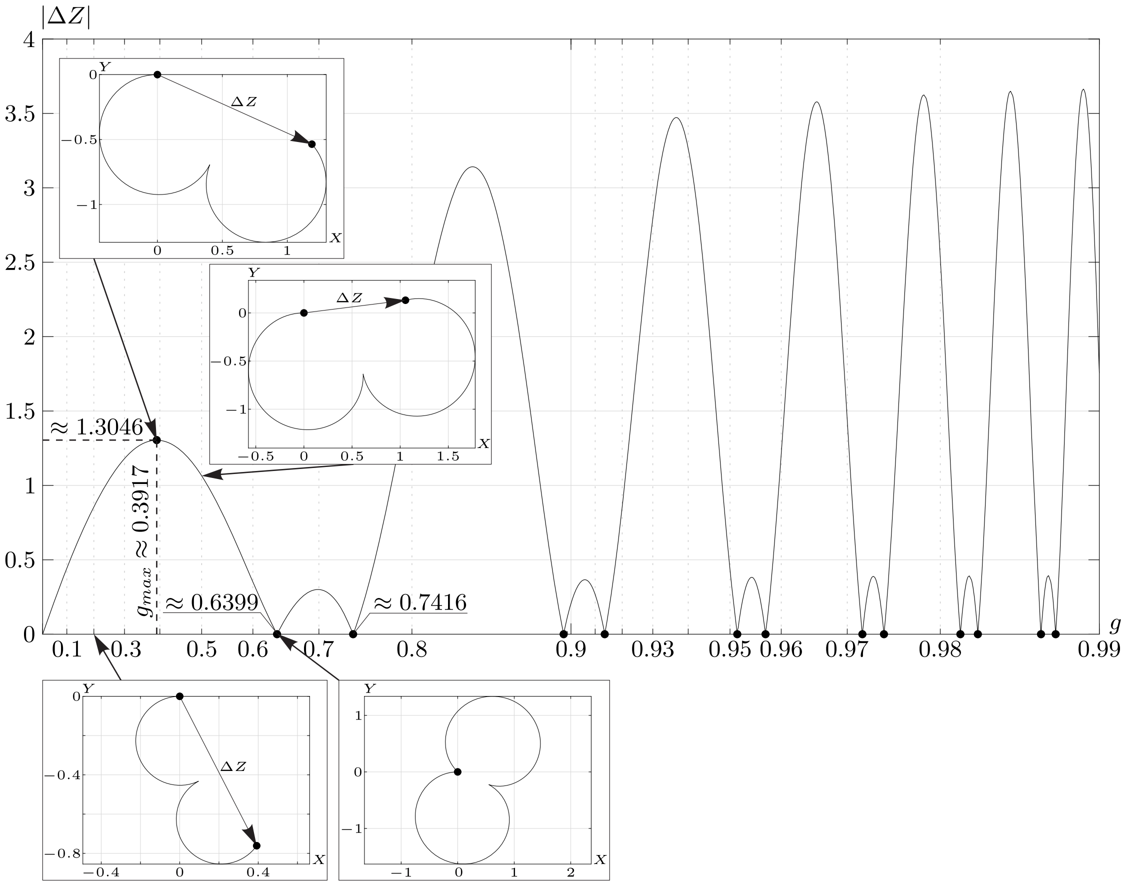

Fig. 8. Dependence of $|\Delta Z|$ on g and examples of trajectories of the geometric center of the foil for the control (45). Parameter values: $m = 1$, $\rho = 1$, $R = 1$, $r = 1.1$, $\vartheta(0) = 0$

another propulsion gait arises. Here, the switching time t_s is found from the condition $p_x(t_s)\Big|_{Q<0,\,\Omega>0} = -mrQ$ and is given by the expression

$$t_s = \frac{2}{\sqrt{|\alpha|}} \arctan \frac{\sqrt{|\alpha|}}{Q}. \tag{53}$$

For the control (52) the linear momenta p_x and p_y change as shown in Fig. 9.

The dependence of the magnitude of displacement $|\Delta Z|$ of the geometric center of the foil for the control law (52) on the parameter g will qualitatively differ from that presented above. This dependence is monotonic (see Fig. 10). However, the trajectories of the foil will be qualitatively similar to those for the preceding gait with the control (45) and have a cusp point corresponding to an abrupt change in the linear momentum.

Remark 5. *If the sign of the angular velocity in the controls* (52) *is reversed:*

$$\begin{gathered} q_1 = -Q\left(\Theta(t) - \Theta(t - t_s)\right) + Q\left(\Theta(t - t_s) - \Theta(t - 2t_s)\right), \quad Q > 0, \\ \omega = -\Omega\left(\Theta(t) - \Theta(t - 2t_s)\right), \quad \Omega > 0 \end{gathered} \tag{54}$$

we obtain a gait similar to that described above.

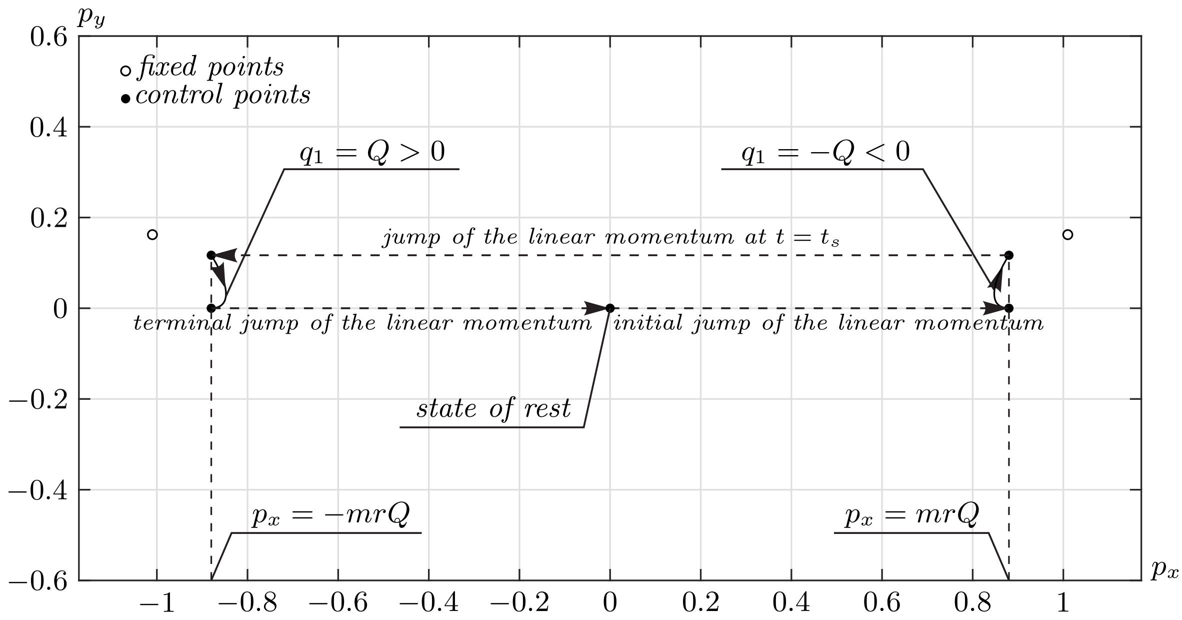

Fig. 9. Changes in the linear momentum vector under the control (52). Parameter values: $m = 1$, $\rho = 1$, $R = 1$, $r = 1.1$, $Q = 0.8$, $\Omega = 1$

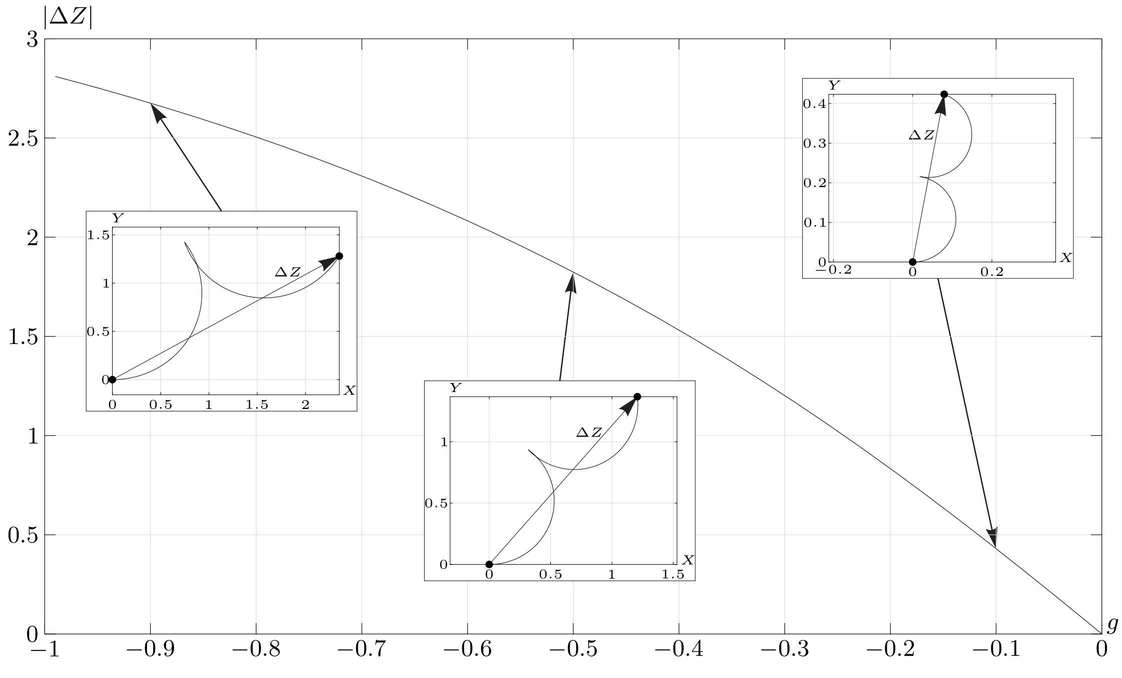

Fig. 10. Dependence of $|\Delta Z|$ on g and examples of trajectories of the geometric center of the foil for the control (52). Parameter values: $m = 1$, $\rho = 1$, $R = 1$, $r = 1.1$, $\vartheta(0) = 0$

4. The last of the propulsion gaits which will be presented in this section arises under the action of the control[5]

$$q_1 = Q\big(\Theta(t) - \Theta(t - t_s)\big) - Q\big(\Theta(t - t_s) - \Theta(t - t_s - T)\big) + Q\big(\Theta(t - t_s - T) - \Theta(t - 2T)\big),$$
$$\omega = \Omega\big(\Theta(t) - \Theta(t - 2t_s)\big) - \Omega\big(\Theta(t - 2t_s) - \Theta(t - 2T)\big). \tag{55}$$

Here, time t_s is found by the formula (46).

Under the action of control (55) the linear momenta p_x and p_y change as shown in Fig. 11. In fact, the gait considered here is a combination of gaits of the two preceding types.

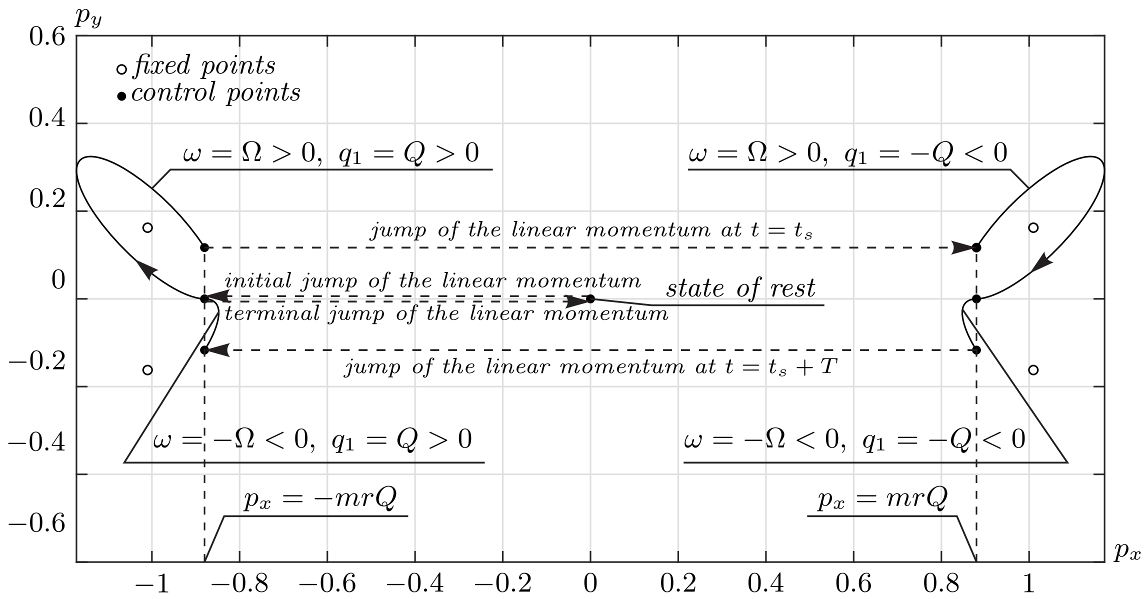

Fig. 11. Changes in the linear momentum vector under the control (55). Parameter values: $m = 1$, $\rho = 1$, $R = 1$, $r = 1.1$, $Q = 0.8$, $\Omega = 1$

Figure 12 shows the dependence of the magnitude of displacement $|\Delta Z|$ on g. We see that this dependence has no zeroes for $g > 0$, i.e., no periodic trajectories arise under the action of control (55). We note that, for the control (55), the trajectories will have an inflexion point (see examples in Fig. 12). This point corresponds to reversal of the sign of the angular velocity.

The propulsion gaits presented above are performed by using both control actions (simultaneous rotation of the rotor and the work of the source/sink that performs either the fluid discharge of the fluid intake). Some of the proposed propulsion gaits imply that the intensity of the source changes sign, which physically corresponds to switching from discharge of the fluid to intake and vice versa. In the last of the proposed gaits, use is also made of the reversal of the angular velocity, which implies a change of the direction of rotation of the rotor.

[5]This control law is obtained if we set $M = 4$, $Q_1 = Q_4 = Q$, $Q_2 = Q_3 = -Q$, $\Omega_1 = \Omega_2 = \Omega$, $\Omega_3 = \Omega_4 = -\Omega$, $\tau_1 = 0$, $\tau_2 = t_s$, $\tau_3 = 2t_s$, $\tau_4 = t_s + T$, $\tau_5 = 2T$ in (13).

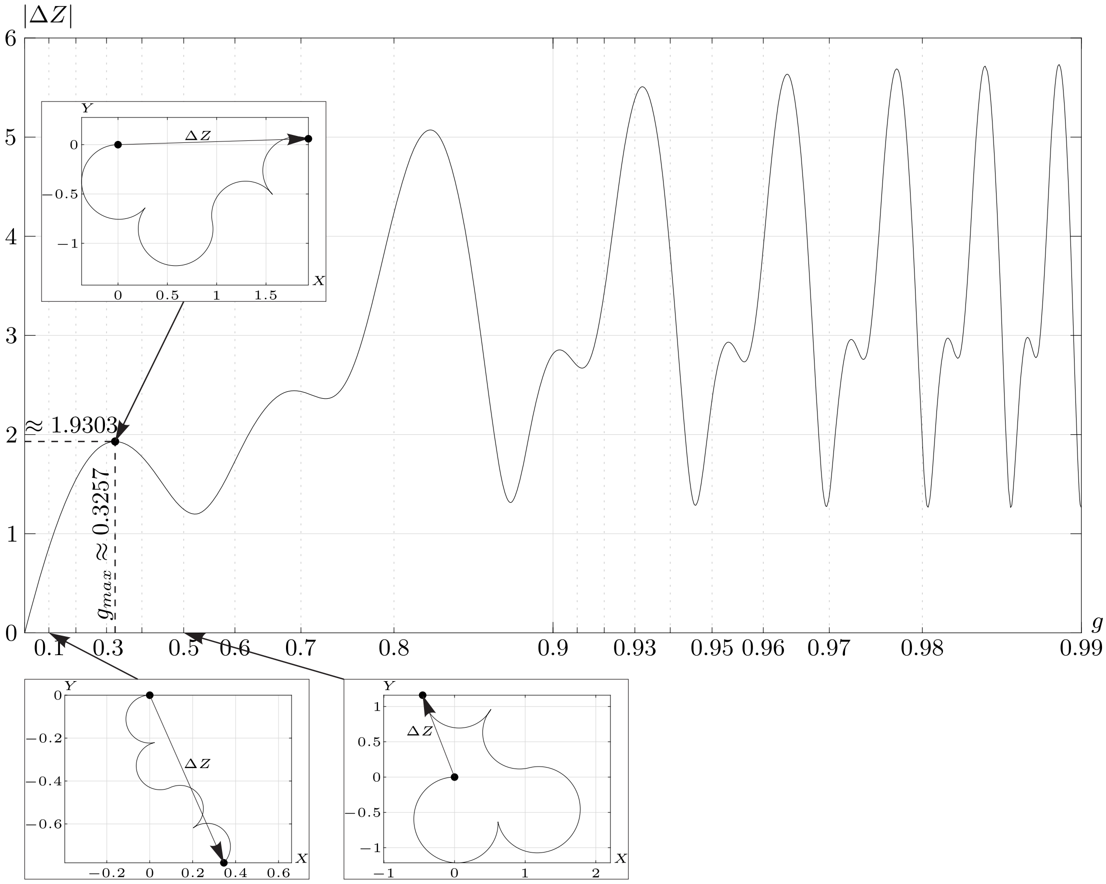

Fig. 12. Dependence of $|\Delta Z|$ on g and examples of trajectories of the geometric center of the foil for the control (55). Parameter values: $m = 1$, $\rho = 1$, $R = 1$, $r = 1.1$, $\vartheta(0) = 0$

5. Control algorithm

The turning and propulsion gaits discussed in Sections 4.2 and 4.3 allow one to construct an algorithm for controlling the motion of the foil in a neighborhood of the prescribed trajectory, which solves the problem formulated in Section 1. We recall that in the hyperbolic case (see Section 3) it is not possible to implement the on-the-spot-turn gait. In addition, a propulsion gait is only possible under the restriction (33) on the values of the system's parameters. Therefore, in what follows the hyperbolic case will not be used in constructing the control algorithm.

Suppose we are given a trajectory $\gamma: \ (X(s), Y(s))$, where s is the parameter of the curve in the neighborhood of which it is necessary to move the foil from the initial point to the terminal point. Choose in some way points $X_j = X(s_j)$, $Y_j = Y(s_j)$ on the curve γ. The transfer between the neighboring points can be performed by means of any of the above-mentioned propulsion gaits, i.e., controls of the form (40), (45), (52) or (55). However, the distance between these points must not exceed some limiting value defined by the chosen gait and the system's parameters. In particular, we will consider only the values $g \leqslant g_{max}$.

To define the control parameters Q and Ω, we need to solve the nonlinear equation

$$|\Delta Z(g_j)| = \sqrt{(X_{j+1} - X_j)^2 + (Y_{j+1} - Y_j)^2} \tag{56}$$

for g_j. Since $|\Delta Z|$ depends on the ratio $g = Q/\Omega$, the propulsion gait can be performed by choosing an arbitrary value of the angular velocity $\Omega = \Omega_j$. Then the intensities are $Q_j = g_j\Omega_j$.

After defining the control parameters Q_j and Ω_j it is necessary to reorient the foil for propulsion in the required direction. To find the orientation of the foil, we need to solve the equation

$$\arg \Delta Z(\vartheta_j)\Big|_{g=g_j} = \arg\left((X_{k+1} - X_k) + i(Y_{k+1} - Y_k)\right). \tag{57}$$

The foil can be turned to the required position using the turning gait described in Section 4.2.

As one of the examples we specify the following trajectory of motion:

$$X = a\cos s, \quad Y = b\sin s, \quad s \in \left[0, \frac{\pi}{2}\right], \quad s\Big|_{t=0} = 0, \tag{58}$$

which we break down into four parts. Figure 13 shows the trajectories followed by the foil using various propulsion gaits.

The use of control (40) for performing a propulsion gait leads to generation of a spiral shaped trajectory. The foil deviates from the prescribed trajectory by a distance commensurable with its length. The trajectory closest to the prescribed one is generated by the control (55).

As another example we define the following trajectory:

$$X = a\cos s, \quad Y = b\sin 3s, \quad s \in [0, 1.9\pi], \quad s\Big|_{t=0} = 0. \tag{59}$$

Figure 14 shows the foil's trajectories generated by various propulsion gaits.

It can be seen from Fig. 14 that the proposed approach using the controls (45), (52), (55) for propulsion ensures the motion of the foil even in a neighborhood of complex trajectories.

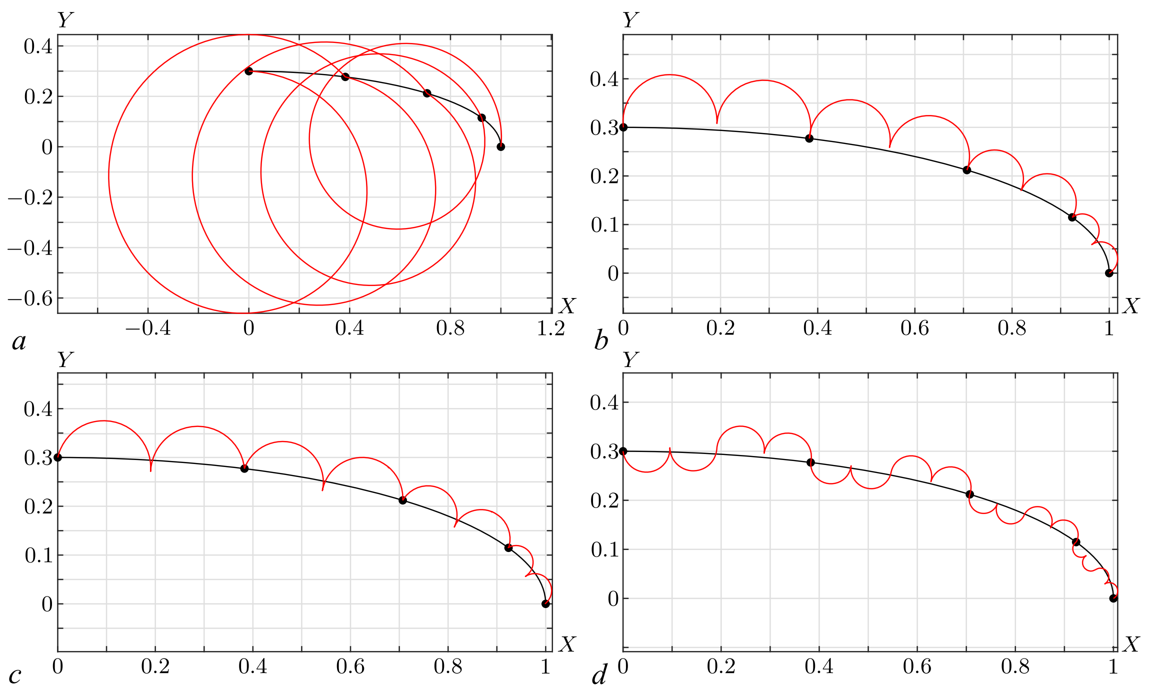

Fig. 13. Trajectories generated by (a) control (40), (b) control (45), (c) control (52), (d) control (55) in a neighborhood of the curve (58). Parameter values: $m = 1$, $\rho = 1$, $R = 1$, $r = 1.1$

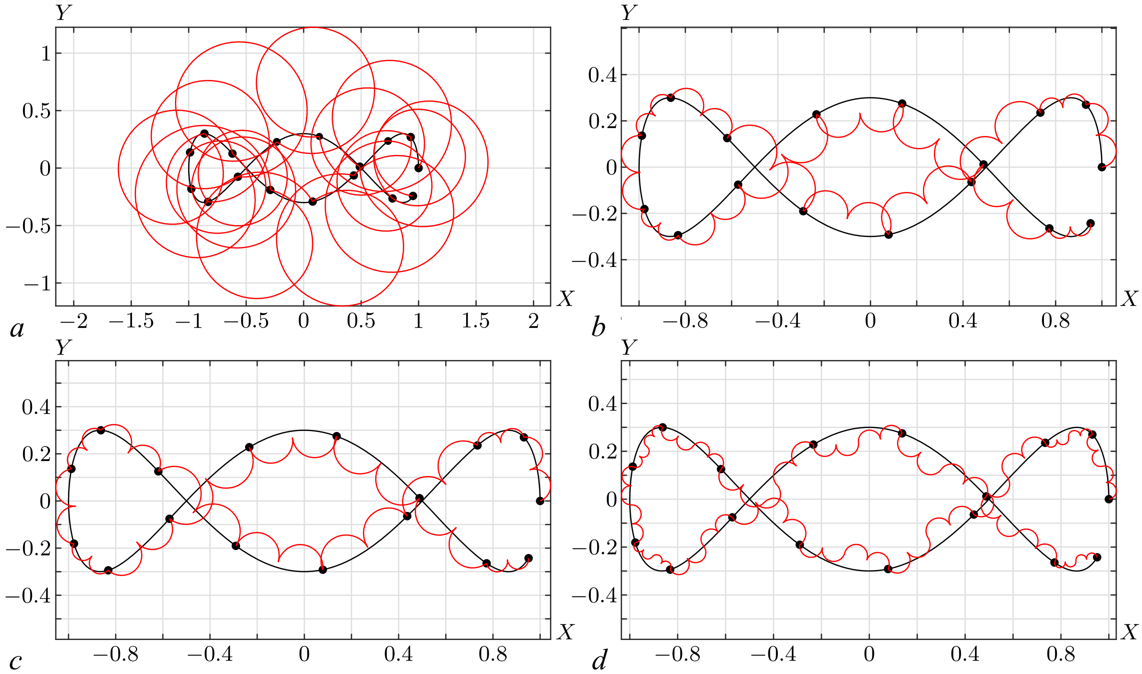

Fig. 14. Trajectories generated by (a) control (40), (b) control (45), (c) control (52), (d) control (55) in a neighborhood of the curve (59). Parameter values: $m = 1$, $\rho = 1$, $R = 1$, $r = 1.1$

Conclusion

The algorithm presented in this paper for controlling the motion of a balanced circular foil in a neighborhood of the prescribed trajectory is based on piecewise constant changes in the intensity of the attached source and the angular velocity. Despite the simplicity, the use of such controls has allowed the solution of the problem considered to be reduced to analysis of explicit solutions of the equations of motion.

The analysis made in this paper can be easily generalized to the case of several attached sources, which also leads to integration of the system of linear differential equations with constant coefficients with respect to the velocities and to explicit quadratures for the trajectory of motion.

Our work suggests the following avenues for further research:

1. The study of the controllability of a balanced circular foil in the case of piecewise smooth controls.
   This problem will reduce to analysis of an inhomogeneous system of linear differential equations with variable coefficients such that its solution can be constructed in the form of quadratures or numerically. The first step of the analysis will be to establish restrictions on the control parameters that ensure a stop when they are switched off, and to construct the dependence of ΔZ on these parameters. Further solution of the problem of the trajectory control and a constructive proof of controllability can be obtained in the same way as it was done in this work.
   We note that smooth controls can be constructed in different ways, for example, in the form of piecewise polynomials in the class of functions C^1 and of higher smoothness, on the basis of trigonometric functions, and in the form similar to (13):

$$\begin{pmatrix} q_1 \\ \omega \end{pmatrix} = \sum_{j=1}^{M} \begin{pmatrix} Q_j \\ \Omega_j \end{pmatrix} \frac{\tanh(k(t-\tau_j)) - \tanh(k(t-\tau_{j+1}))}{2}, \quad Q_j = \mathrm{const}, \quad \Omega_\mathrm{j} = \mathrm{const},$$

Here, the parameter k regulates the smoothness of switching of the intensities of control actions. It is expected that, for $k \gg 1$, the results will be similar to those obtained in this paper.

2. Analysis of the controllability of an unbalanced circular foil and noncircular foils, for example, an elliptic foil.
   The solution of these problems leads to analysis of a system of nonlinear differential equations whose explicit form for a circular foil is presented in Section 1. To derive the equations of motion for noncircular foils, it is necessary to calculate the complex potential of fluid motion and to find the force and the pressure torque acting on the body.
   Analysis of controllability for these problems (regardless of the choice of the form of the control actions) will also reduce to solving the problem of a stop during the switching-off of the controls, to searching for elementary gaits and to constructing the dependence of ΔZ on the control parameters.
3. Investigation of the efficiency of the proposed control algorithm according to some quality criterion (motion time or energy minimization) under possible restrictions on the intensities. We note that this problem can be solved using the approach discussed in [16].
4. Incorporation of dissipative and inertial properties of the medium into the mathematical model.
   The mathematical model of this problem can be based on the inclusion of the terms [17] that are linear or quadratic in velocities into the equations of motion.

References

1. Vetchanin EV, Valieva AR. Analysis of the force and torque arising during the oscillatory motion of a Joukowsky foil in a fluid. Rus. J. Nonlin. Dyn. 2024;20(1):79–93. DOI: 10.20537/nd231210.
2. Borisov AV, Kuznetsov SP, Mamaev IS, Tenenev VA. Describing the motion of a body with an elliptical cross section in a viscous uncompressible fluid by model equations reconstructed from data processing. Tech. Phys. Lett. 2016;42:886–890. DOI: 10.1134/S1063785016090042.
3. Anisimov VD, Egorov AG, Nuriev AN, Zaitseva ON. Propulsive motion of cylindrical vibration-driven robot in a viscous fluid. Scientific Notes of Kazan University. Series of Physical and Mathematical Sciences. 2024;166(3):277–296. DOI: 10.26907/2541-7746.2024.3.277-296.
4. Borisov AV, Mamaev IS, Ramodanov SM. Motion of a circular cylinder and n point vortices in a perfect fluid. Regul. Chaotic Dyn. 2003;8(4):449–462. DOI: 10.1070/RD2003v008n04ABEH000257.
5. Mamaev IS, Bizyaev IA. Dynamics of an unbalanced circular foil and point vortices in an ideal fluid. Physics of Fluids. 2021;33:087119. DOI: 10.1063/5.0058536.
6. Artemova EM, Vetchanin EV. Control of the motion of a circular cylinder in an ideal fluid using a source. Bulletin of Udmurt University. Mathematics. Mechanics. Computer Science. 2020;30(4):604–617. DOI: 10.35634/vm200405.
7. Artemova EM, Vetchanin EV. The motion of an unbalanced circular disk in the field of a point source. Regul. Chaotic Dyn. 2022;27(1):24–42. DOI: 10.1134/S1560354722010051.
8. Artemova EM, Vetchanin EV. The motion of a circular foil in the field of a fixed point singularity: Integrability and asymptotic behavior. Physics of Fluids. 2024;36:027139. DOI: 10.1063/5.0185865.
9. Artemova EM, Lagunov DA, Vetchanin EV. The motion of an elliptic foil in the field of a fixed vortex source. Rus. J. Nonlin. Dyn. 2025;21(2):135–155. DOI: 10.20537/nd241203.

10. Kilin AA, Gavrilova AM, Artemova EM. Dynamics of an elliptic foil with an attached vortex in an ideal fluid: The integrable case. Regul. Chaotic Dyn. 2025;30:931–951. DOI: 10.1134/S1560354724590015.
11. Kochin, NE, Kibel IA, Roze NV. Theoretical Hydrodynamics. New York: Wiley; 1964. 577 p.
12. Milne-Thomson LM. Theoretical Hydrodynamics. London: Macmillan; 1962. 660 p.
13. Sedov LI. Two-Dimensional Problems in Hydrodynamics and Aerodynamics. New York: Wiley; 1965. 427 p.
14. Korotkin AI. Added Masses of Ship Structures. Dordrecht: Springer; 2009. 392 p. DOI: 10.1007/978-1-4020-9432-3.
15. Borisov AV, Mamaev IS. Rigid Body Dynamics. Berlin: De Gruyter; 2019. 526 p. DOI: 10.1515/9783110544442.
16. Ardentov AA. Extremals in the Markov-Dubins problem with control on a triangle. Rus. J. Nonlin. Dyn. 2024;20(1):27–42. DOI: 10.20537/nd231207.
17. Kuznetsov SP. Motion of a falling card in a fluid: Finite-dimensional models, complex phenomena, and nonlinear dynamics. Rus. J. Nonlin. Dyn. 2015;11(1):3–49. DOI: 10.20537/nd1501001.